Special Section on Pediatric Drug Disposition and Pharmacokinetics

Predicting Stereoselective Disposition of Carvedilol in Adult and Pediatric Chronic Heart Failure Patients by Incorporating Pathophysiological Changes in Organ Blood Flows–A Physiologically Based Pharmacokinetic Approach Ⓢ

Muhammad Fawad Rasool, Feras Khalil, and Stephanie Läer

Department of Clinical Pharmacy and Pharmacotherapy, Heinrich-Heine University, Düsseldorf, Germany (M.F.R., F.K., S.L.); and Faculty of Pharmacy, Bahauddin Zakariya University, Multan, Pakistan (M.F.R.)

ABSTRACT

Chronic heart failure (CHF) is a systemic low perfusion syndrome resulting from impairment in the pumping function of the heart. The decrease in blood supply to body organs can potentially affect the pharmacokinetics (PK) of the drugs being administered. Carvedilol is administered as a racemic mixture and undergoes extensive stereoselective first pass metabolism. For such a drug, the pathophysiological changes occurring in CHF can have a profound impact on PK, and thus the resulting pharmacodynamic response, of both enantiomers. The aim of the current work was to predict stereoselective disposition of carvedilol after incorporating the pathophysiological changes in CHF into a whole-body physiologically based PK model using Simcyp, and to scale that model to pediatric CHF patients on a physiologic basis to investigate whether the same changes in the adult model can also be adopted for children. The developed model has successfully described PK of carvedilol enantiomers in healthy adults and in patients after the incorporation of reduced organ blood flows, as seen by the visual predictive checks and the calculated observed/predicted ratios for all PK parameters of interest. In contrast to adults, pediatric patients up to 12 years of age were better described without the reductions in organ blood flow, whereas older pediatric patients were better described after incorporating organ blood flow reductions. These findings indicate that the incorporated blood flow reductions in the adult model cannot be directly adopted in pediatrics, at least for the young ones; however, to draw definite conclusions, more data are still needed.

Introduction

Chronic heart failure (CHF) is a systemic low perfusion syndrome resulting from impairment in the pumping function of the heart, leading to a decrease in the blood supply to various body organs and having a potential to affect the pharmacokinetics (PK) of administered drugs (Ogawa et al., 2013; Yancy et al., 2013). In CHF, the reduced blood flows to the gastrointestinal tract, the peripheral tissues, as well as the liver and the kidneys can affect the drug absorption, distribution, metabolism, and elimination (ADME) (Berkowitz et al., 1963; Zelis et al., 1975; Sica, 2003; Ogawa et al., 2013). These reductions in the organ blood flows are associated with the severity of disease (Leithe

et al., 1984). The New York Heart Association (NYHA) functional classification of heart failure (NYHA class) is used for categorizing heart failure patients with respect to severity of disease, starting from compensated, mild (NYHA I) to decompensated, severe (NYHA IV) CHF (Criteria Committee of the New York Health Association, 1994). In compensated heart failure, there is no significant impact on PK of the administered drugs, whereas ~50% reduction in clearance (CL) of drugs has been observed in decompensated CHF (NYHA III and IV) (Ogawa et al., 2013). The organ blood flow reductions in heart failure can be correlated with NYHA class of the patients, and hence can be used to understand and predict the PK of drugs being administered in patients with heart failure.

Racemic drugs are composed of enantiomers that can differ greatly in their PK and pharmacodynamic properties (Birkett, 1989). The PK differences between the enantiomers are mainly due to differences in absorption and disposition that can lead to variations in their systemic concentrations and hence can influence the concentration-effect

ABBREVIATIONS: ADME, absorption, distribution, metabolism, and elimination; $AUC_{0-\infty}$, area under the systemic drug concentration-time curve from time 0 to infinity; BCS, Biopharmaceutics Classification System; C_{max}, maximal systemic drug concentration; CHF, chronic heart failure; CL, clearance; CL/F, CL after the oral application; CL_{int}, total hepatic intrinsic CL; CL_{perm}, permeability CL; EM, extensive metabolizer; F, bioavailability; f_a, fraction absorbed; F_h, fraction of drug escaping the hepatic metabolism; $f_{u,Gut}$, unbound fraction of the drug in the enterocyte; NYHA, New York Heart Association; PBPK, physiologically based PK; $P_{eff,man}$, human jejunum permeability; P-gp, P-glycoprotein; PK, pharmacokinetics; PM, poor metabolizer; Q_H, hepatic blood flow; Q_{villi}, villous blood flow; ratio(Obs/Pred), observed/predicted ratio.

relationship (Tucker and Lennard, 1990). Because some of the enantiomers show stereoselective disposition, any pathophysiological condition that can affect their CL can have a profound impact on their exposure and efficacy. Carvedilol is a racemic mixture of two enantiomers, with S-enantiomer having both α_1-receptor–blocking and β-adrenoreceptor–blocking activities, whereas R-enantiomer is more selective toward α_1-receptor–blocking activity (Neugebauer et al., 1990). Both enantiomers undergo extensive stereoselective first-pass metabolism through CYP enzymes (CYP2D6, CYP1A2, CYP2C9, CYP3A4, and CYP2E1) and UGT enzymes (UGT1A1, UGT2B4, and UGT2B7) (Oldham and Clarke, 1997; Ohno et al., 2004; Takekuma et al., 2012), with reported absolute bioavailability (F) of 31.1% for R-carvedilol and 15.1% for S-carvedilol (Neugebauer et al., 1990). Because CYP2D6 is the main metabolic enzyme that is involved in the metabolism of both enantiomers and is more selective toward the overall disposition of R-carvedilol, the decrease activity of this enzyme in poor metabolizers (PMs) may result in higher systemic concentration of R-carvedilol and hence an increase in α-blockade, which can cause acute blood pressure reduction and increased incidence of orthostatic hypotension in comparison with extensive metabolizers (EMs) of CYP2D6 (Zhou and Wood, 1995). Because carvedilol is used in the management of CHF and it undergoes extensive stereoselective first-pass metabolism, the organ blood flow reductions occurring in CHF can significantly affect its ADME.

A physiologically based PK (PBPK) model incorporating reduced hepatic and renal blood flows has been used previously to predict PK of racemic carvedilol in adult and pediatric CHF patients (Rasool et al., 2015). However, the reductions in blood flow to limbs, adipose, skin, and muscle tissues, which can additionally affect the drug distribution and hence the plasma concentration of the drug, were not yet incorporated in the previously reported carvedilol-CHF model (Rasool et al., 2015). Keeping in mind that carvedilol is administered as a racemic mixture of R and S enantiomers, which have ~twofold difference in their F, the organ blood flow reductions occurring in CHF can affect the disposition of both in a stereoselective fashion. The differences in the exposures of R- and S-carvedilol will influence the expected pharmacodynamic response and may potentially lead to adverse drug reactions. A PBPK model that incorporates all the reported relevant blood flow reductions occurring in CHF can be used to predict stereoselective disposition of carvedilol in CHF patients. Furthermore, a developed and evaluated PBPK model with clinical data in adult CHF patients can be scaled to pediatrics on physiologic basis by using a population-based ADME simulator.

The main objective of this work was to develop a PBPK drug-disease model capable of predicting stereoselective disposition of carvedilol in CHF patients after incorporating the relevant organ/tissue blood flow changes and to evaluate it with the available clinical data in adult and pediatric CHF patients.

Materials and Methods

Modeling Platform

The population-based PBPK simulator, Simcyp version 14.1 (Simcyp, Sheffield, UK), was used in developing a whole-body PBPK model.

Modeling Strategy

A PBPK model was developed by adopting a systematic model-building strategy (Khalil and Laer, 2014), starting with the literature search for screening of drug-specific input parameters and clinical PK data to be used in model development. This was followed by incorporation of these data into the simulator and selection of system parameters for running predictions in virtual populations and the final evaluation of the developed model with the

comparison of predicted results with the observed clinical trial data. To avoid the complexity associated with the oral drug absorption, initially predictions were performed after i.v. drug application and all the drug-specific parameters that can potentially influence drug disposition, such as in vivo CL and contributions of various metabolic enzymes (CYPs and UGTs), were optimized. After successful evaluation of the i.v. predictions with the observed data, the previously selected parameters are kept constant and other additional drug-specific parameters that can affect drug absorption process, such as permeability and fraction unbound of the drug in the enterocyte, are selected or optimized. Among the seven PK data sets (two i.v. and five oral) in healthy adults, three data sets (one i.v. and two oral) were used for model building, remaining data sets were used for model verification, and all the data sets were used for model evaluation. After evaluation of developed model in healthy adults, pathophysiological changes in organ blood flows occurring in CHF were incorporated to predict ADME of carvedilol enantiomers in adult CHF patients. After successful evaluation of developed CHF model with the observed data, it was scaled to pediatrics on a physiologic basis by using the pediatric module of Simcyp. To see the impact of reduced organ blood flows on the model predictions in pediatric CHF patients, simulations were performed in duplicate, that is, with and without incorporating reductions in organ blood flows.

All of the predictions were performed by creating a virtual population with same demographics as in the original trial by keeping the age range, proportion of females, fluid intake, fasting/fed states, and, where applicable, same genotypic frequencies. In adults, all the predictions were performed by creating a virtual population of 100 individuals for every PK data set. In pediatrics, the initial simulations were performed in the entire age range, including the young adult, without stratifying them in different age groups, by creating a virtual population of 1000 individuals within the age range of 0.12–19.3 years. This was followed by simulating pediatric patients in different age groups by creating a virtual population of 100 individuals for every age group. The workflow for the development of PBPK model can be seen in Fig. 1.

PBPK Model Parameterization

After undergoing an extensive literature search, relevant in vivo and in vitro drug- and population-specific data were selected for completing the model parameterization. The final model input parameters are summarized in Table 1. The detailed parameterization of various drug- and disease-specific components used in the final PBPK model is given below.

Absorption

To predict oral drug absorption, the advanced, dissolution, absorption, and metabolism model was used (Jamei et al., 2009). The human jejunum permeability ($P_{eff,man}$) of R-carvedilol was predicted using in vitro Caco-2 permeability (P_{app}) input data after calibrating it with reference value of atenolol within Simcyp (Tian et al., 2012). For S-carvedilol, the $P_{eff,man}$ was optimized and adjusted manually after sensitivity analysis to get a good visual fit with the observed clinical data. The model $P_{eff,man}$ values for R- and S-carvedilol were 3.9×10^{-4} (cm/s) and 1.6×10^{-4} (cm/s), respectively. The predicted absorbed fractions (f_a) of R- and S-carvedilol were 0.98 and 0.85, respectively, which are in accordance with carvedilol having a high permeability and belonging to Biopharmaceutics Classification System (BCS) class II. Additionally, the unbound fractions of R- and S-carvedilol within the enterocytes ($f_{u,Gut}$) were predicted using Simcyp. Although some reports suggest a possible role of P-glycoprotein (P-gp) in carvedilol disposition (Kaijser et al., 1997; Giessmann et al., 2004), active transport process is considered to be significant only when carvedilol is given concomitantly with other P-gp substrates (Aiba et al., 2005). Furthermore, carvedilol is considered to be a strong inhibitor and not a good substrate to P-gp (Wessler et al., 2013); taking this information into consideration, no active transport data were incorporated in the developed PBPK model.

Distribution

A perfusion limited whole-body full PBPK model was used for predicting enantiomeric distribution of carvedilol. The volumes of distribution at steady state and the tissue to plasma partition coefficients for R- and S-carvedilol were predicted by using Poulin and Theil method with the Bierezhkovskiy correction (Berezhkovskiy, 2004).
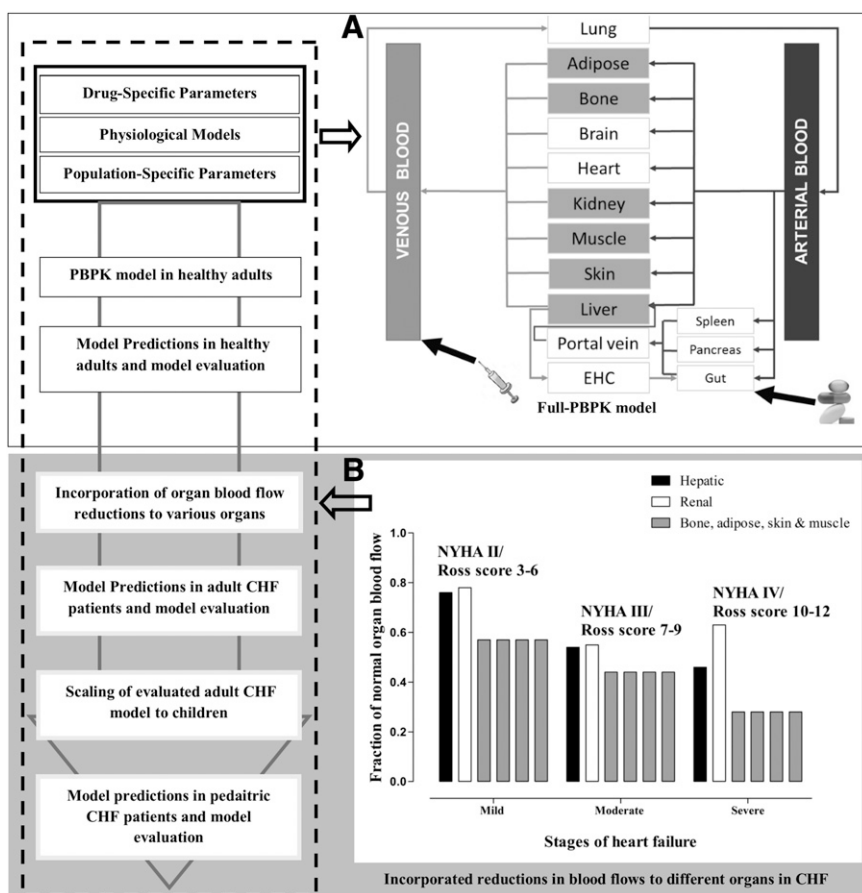
Fig. 1. Workflow for the development of adult and pediatric PBPK heart failure model. The white area shows model development in healthy adults, and the gray shaded area shows stages of model development in CHF patients. (A) Full PBPK model with different body compartments. The gray compartments show the organs in which blood flow reductions are incorporated. (B) Incorporated organ blood flow reductions in CHF patients with respect to severity of disease.

Elimination

Due to absence of relevant metabolic enzyme-specific data that can support and predict the reported enantiomer-specific carvedilol CLs, the intrinsic CLs of metabolic enzymes involved in R- and S-carvedilol CL were back calculated from their respective i.v. CL using the retrograde model for enzyme kinetics in Simcyp (Neugebauer et al., 1990; Cubitt et al., 2011; Salem et al., 2014). To calculate the total hepatic intrinsic CL (CL_{int}), the adult i.v. CL, known fractions of hepatic and renal CL, the fraction of unbound drug (f_u), the blood to plasma drug ratio, and the hepatic blood flow were used as input parameters. The predicted hepatic CL_{int} was further divided and assigned to different CYP enzymes, on the basis of available evidence regarding fractional contributions of these enzymes. The CL_{int} not being assigned to any CYP enzyme was used as additional drug CL in the program. The hepatic intrinsic CL was predicted using the well-stirred liver model (eq. 1), as follows:

$$CL_{int} = \frac{Q_H \times CL_H}{fu_B \times (Q_H - CL_H)} \tag{1}$$

The fractional contributions of CYP enzymes involved in metabolism of R- and S-carvedilol were obtained from available evidences in the published reports (Oldham and Clarke, 1997; Giessmann et al., 2004; Sehrt et al., 2011). It is stated that CYP2D6 is the major metabolic enzyme involved in carvedilol CL with some minor contributions from CYP1A2, CYP2C9, CYP2E1, and CYP3A4. The 74% of total R-carvedilol CL is dependent on CYP2D6, whereas other CYP enzymes have a minor role in its disposition, 50% of total S-carvedilol CL is attributed to CYP2D6, and other metabolic enzymes may have an important role in its overall disposition (Zhou and Wood, 1995; Oldham and Clarke, 1997; Sehrt et al., 2011). In healthy adults, glucuronidation accounts for 20–23% of total carvedilol CL (Neugebauer and Neubert, 1991) and three UGT isoforms, UGT1A1, UGT2B4, and UGT2B7, are involved in its metabolism (Ohno et al., 2004). The contributions of UGT1A1, UGT2B4, and UGT2B7 are reported to be about 30%, 25–40%, and 30–45% for R-carvedilol, and 12–20%, 15–26%, and 60–65% for S-carvedilol, respectively (Takekuma et al., 2012).

Taking into account the above-mentioned information, 80% of total carvedilol CL was assigned to the CYP enzymes (R-carvedilol: 74% CYP2D6, 2% CYP1A2, 2% CYP2C9, 1% CYP3A4, and 1% CYP2E1, and S-carvedilol: 50% CYP2D6, 10% CYP1A2, 10% CYP2C9, 5% CYP3A4, and 5% CYP2E1) using retrograde model, and remaining 20% was assigned to UGT enzymes, which was predicted as additional CL in the program. The UGT-enzyme contributions were optimized manually to achieve good agreement with the observed clinical data. The final values of different CL parameters used in the developed PBPK model are shown in Table 1.

The hepatic CL was predicted by using well-stirred liver model using eq. 2 (Wilkinson and Shand, 1975):

$$CL_H = \frac{Q_H \times fu_B \times CLu_{H,int}}{Q_H + fu_B \times CLu_{H,int}} \tag{2}$$

The reductions in hepatic blood flow (Q_H) occurring in CHF were incorporated into the model for predicting CL of carvedilol enantiomers in CHF patients.

The fraction escaping the gut wall metabolism (F_G) was predicted using eq. 3:

$$F_G = \frac{Q_{Gut}}{Q_{Gut} + f_{u,Gut} \times CL_{u,int,Gut}} \tag{3}$$

where $f_{u,Gut}$ is the unbound fraction of the drug in the enterocyte, $CL_{u,int,Gut}$ intrinsic CL in the gut, and Q_{Gut} is a hybrid term predicted by using villous blood flow (Q_{villi}) and the permeability CL (CL_{perm}), which is measured from the effective permeability of the compound. Q_{Gut} is calculated by using eq. 4:

$$Q_{Gut} = \frac{Q_{villi} \times CL_{perm}}{Q_{villi} + CL_{perm}} \tag{4}$$

The oral bioavailability was predicted by using eq. 5:

$$F = f_a \times F_g \times F_h \tag{5}$$

TABLE 1
The drug-dependent parameters and characteristics of the presented PBPK model

Parameter	R-Carvedilol	S-Carvedilol	Source/ Reference (R, S)
Molecular weight (g/mol)	406.47	406.47	PubChem.
$LogP_{o:w}$	4.19	4.19	PubChem.
pK_a	7.97	7.97	(Caron et al., 1999)
Absorption			
Model		ADAM	
Solubility (mg/mL)[a]	0.01	0.01	(Benet et al., 2011)
$P_{eff,man}$ (cm/s)	3.9×10^{-4}[b]	1.6×10^{-4}	(Tian et al., 2012), Sensitivity analysis and manual optimization
$f_{u,Gut}$	0.00138	0.00124	Simcyp predicted
Q_{Gut} (L/h)[c]	12.2	8.1	Simcyp predicted
Distribution			
Model		Full PBPK	
V_{ss} (L/kg)—predicted	1.57	1.95	Poulin and Theil method
V_{ss} (L/kg)— observed	1.39–3.40	1.42–3.84	(Neugebauer et al., 1990)
Blood to plasma ($B:P$) ratio	0.67	0.74	(Fujimaki et al., 1990)
fu_P	0.0045	0.0063	(Fujimaki et al., 1990)
Elimination			
CL_{iv} (L/h)—used as input in retrograde model	41	54	(Neugebauer et al., 1990), Optimized
CYP2D6 CL_{int} (μL/min/mg/pmol isoform)[d]	656.5	702.2	Simcyp retrograde model of enzyme kinetics[d,e]
CYP1A2 CL_{int} (μL/min/mg/pmol isoform)[d]	2.7	21.6	
CYP2C9 CL_{int} (μL/min/mg/pmol isoform)[d]	1.9	15.3	
CYP3A4 CL_{int} (μL/min/mg/pmol isoform)[d]	0.5	4.1	
CYP2E1 CL_{int} (μL/min/mg/pmol isoform)[d]	1.1	9.2	
UGT1A1 CL_{int} (μL/min/mg/pmol isoform)[e]	8.8	9.1	
UGT2B4 CL_{int} (μL/min/mg/pmol isoform)[e]	10.5	10.4	
UGT2B7 CL_{int} (μL/min/mg/pmol isoform)[e]	8.9	19.6	
CL_R (L/h)[f]	0.25	0.25	(Gehr et al., 1999)

ADAM, advanced, dissolution, absorption, and metabolism; CL_{int}, intrinsic clearance; CL_{iv}, i.v. clearance; CL_R, renal clearance; $f_{u,Gut}$, fraction unbound drug in enterocytes; fu_P, fraction of unbound drug in plasma; $LogP_{o:w}$, octonal-water partition coefficient; pK_a, acid dissociation constant; Q_{Gut}, hybrid term derived from villous blood flow and drug permeability through the enterocyte membrane.
[a]Assumed to be similar for both enantiomers.
[b]Human jejunum permeability calculated from P_{app} value of a Caco-2 assay by calibrating with atenolol and using Simcyp.
[c]Q_{gut} value was adjusted according to decrease in hepatic blood flow in CHF patients; see *Materials and Methods* for details.
[d]Values calculated by using retrograde model in Simcyp.
[e]Values calculated manually by predicted additional clearance using retrograde model in Simcyp.
[f]Assumed to be similar in both enantiomers.

where f_a is the fraction of drug absorbed, F_g is the fraction of drug that escapes metabolism in the gastrointestinal tract, and F_h is the fraction of drug that escapes the hepatic metabolism.

Pediatric PBPK Model

When the developed PBPK was able to predict ADME of both R- and S-carvedilol in adult healthy and CHF patients, it was scaled to pediatrics on a physiologic basis using the pediatric module of Simcyp. This module includes a wide variety of relevant age-specific physiologic and anatomic parameters that facilitate the pediatric scaling of drug CL on a physiologic basis. These parameters include the age-related changes in total body composition, plasma protein binding, blood volume, organ blood flows, and abundance of different metabolic enzymes (Johnson and Rostami-Hodjegan, 2011). In pediatric module, the renal function is described on the basis of glomerular filtration rate, which is linked with BSA of the simulated individuals (Johnson et al., 2006). To simulate the oral drug absorption process in pediatrics, the β-version of the pediatric advanced, dissolution, absorption, and metabolism model was used with the similar input value of mean gastric emptying time as in the adult model (0.4 hour).

To assess the uncertainty associated with some pediatric model input parameters, which were adopted from adult PBPK model, sensitivity analysis was performed. The details of the sensitivity analysis are described in the supplemental file (Supplemental Material).

Because all of the pediatric patients included in model evaluation were diagnosed with CHF, the organ blood flow reductions were incorporated in the pediatric model to see impact of blood flow reductions on ADME of R- and S-carvedilol.

Blood Flow Changes to Different Organs/Tissues in Heart Failure

The blood flow to liver and kidney decreases with increasing severity of heart failure, and it has been quantified previously (Leithe et al., 1984). The quantified fractional reduction in blood flow was 0.76, 0.54, and 0.46 of normal hepatic flow in mild, moderate, and severe CHF patients, whereas the reduction in renal blood flow was not linear when moving from moderate to severe CHF, as the reported

fractional decrease was, 0.78, 0.55, and 0.63 of normal blood flow in mild, moderate, and severe CHF patients (Leithe et al., 1984). Furthermore, the changes in blood flow to limbs can affect the drug distribution, as the blood flow to the limbs also supplies skin, adipose, muscle, and bone (Lee et al., 1993). The quantified fractional reduction in limb blood flow was 0.57, 0.44, and 0.28 of normal limb blood flow in mild, moderate, and severe CHF patients (Leithe et al., 1984).

The NYHA functional classification system for CHF can be directly correlated with the reported reductions in different organ blood flows, by categorizing mild CHF patient in NYHA class II, moderate CHF patient in NYHA class III, and severe CHF patient in NYHA class IV (Leithe et al., 1984; Criteria Committee of the New York Health Association, 1994). All of these organ/tissue blood flow reductions were incorporated within the simulated virtual populations by decreasing the cardiac output to these organs within Simcyp.

In CHF patients there is hepato-splanchnic congestion, affecting the passive drug diffusion that results in decreased migration of drug from the intestinal lumen into systemic circulation, which is depicted as decrease in f_a of the drug (Sica, 2003). Furthermore, the gastrointestinal absorption of drugs having low solubility like carvedilol (0.01 mg/mL, BCS II) is more sensitive to CHF-associated changes occurring in gut blood flow (Ogawa et al., 2014). Because in the developed model the reduction in blood flow to gut was accounted by reducing the Q_H (both arterial and portal) and to account for decrease in Q_{villi} with severity of CHF, the predicted Q_{Gut} (eq. 4) value due to its dependence on Q_{villi} was reduced in accordance with the reduction in hepatic blood flow.

Keeping in mind the reliance of NYHA functional classification system on assessment of physical activity in CHF patients and difficulty of assessing physical activity in pediatrics, NYHA functional classification of CHF is not generally used in pediatric patients and as an alternative Ross scoring method is used to assess the severity of CHF in pediatric patients (Ross et al., 1992). In Ross score system, a score of 0–2 categorizes the patient as asymptomatic, 3–6 as with mild CHF, 7–9 as with moderate CHF, and 10–12 as a patient with severe CHF (Ross et al., 1992; Laer et al., 2002). Because there is no report of a clinical study quantifying the changes in the organ/tissue blood flow in pediatric patients, the organ blood flow reductions in pediatrics were assumed to be similar as in adult

CHF patients (Leithe et al., 1984). The incorporated organ blood flow reductions with respect to severity of CHF in adults (NYHA class) and in pediatric patients (Ross score) are shown in Fig. 1.

PK/Clinical Data

Healthy and Adult Patients with CHF. MEDLINE database was searched for screening and identification of PK studies of R- and S-carvedilol in healthy adults and CHF patients with known demographic information and reported systemic drug concentration-time profiles. As a result of the search, systemic drug concentration-time data from five different clinical studies in healthy adults (4 studies and 36 subjects) and CHF patients (one study, 10 patients with NYHA III and 10 patients with NYHA IV, 4 PK data sets) were used in the adult model development and evaluation (Neugebauer et al., 1990; Spahn et al., 1990; Zhou and Wood, 1995; Tenero et al., 2000; Behn, 2001). These studies provided a total of 11 data sets (7 data sets in healthy and 4 data sets in CHF patients) (Table 2). Each PK data set used for model development and evaluation represents a mean or median observed concentration-time profile after i.v. or oral doses of R- and S-carvedilol. Among the data sets used, one was provided by the author (Behn, 2001) and the rest were scanned from the publications' figures (Neugebauer et al., 1990; Spahn et al., 1990; Zhou and Wood, 1995; Tenero et al., 2000) using the "digitizer" tool in software OriginPro version 9.0 (OriginLab, Northampton, MA). CYP2D6-specific genotype data were available in two clinical studies (Zhou and Wood, 1995; Behn, 2001).

Pediatric Patients with CHF. One clinical PK data set, including 15 pediatric CHF patients and one young adult with known age, gender, height, weight, CYP2D6 genotype, dose, Ross score, and measured systemic drug concentration-time profiles, was used (Table 3) (Behn, 2001). The age of the patients ranged from 43 days to 19.3 years (average: 6.7 years) and they received a 0.09 mg/kg dose of oral R- and S-carvedilol. The pediatric patients were divided into different age groups, that is, infant (1 month–1 year), young child (2–6 years), children (6–12 years), and adolescents (12–18 years), according to guidelines set by World Health Organization (http://archives.who.int/eml/expcom/children/Items/PositionPaperAgeGroups.pdf).

Model Evaluation. The evaluation of PBPK model was performed by visual predictive checks and comparison of observed and predicted PK parameters. The visual predictive checks were performed by overlaying the observed systemic drug concentration-time profile on the median predicted values along with the minimum/maximum, 5th and 95th percentiles of the predictions.

The PK parameters were compared by performing a noncompartmental analysis for each observed PK profile and its corresponding predicted value using Phoenix WinNonLin version 6.4 (Certara L.P., Princeton, NJ). The area under the systemic drug concentration-time curve from time zero to infinity ($AUC_{0-\infty}$) was calculated via the linear trapezoidal rule by using best fit method with minimum of three systemic concentration versus time points for estimation of elimination rate constant (k_e). The maximal systemic concentration in a profile was defined as maximal systemic drug concentration (C_{max}), and the CL [CL for the i.v. application, CL after the oral application (CL/F) for the oral application] was calculated by dividing the given dose by the calculated $AUC_{0-\infty}$. The results of noncompartmental analysis were presented as the observed/predicted ratios [ratios$_{(Obs/Pred)}$] of the PK parameters. Moreover, the calculated values of area under the systemic drug concentration-time curve from time 0 to the last measured concentration and $AUC_{0-\infty}$ were compared to see whether there is any significance difference that can impair the results. The ratios$_{(Obs/Pred)}$ for area under the systemic drug concentration-time curve from time 0 to the last measured concentration and $AUC_{0-\infty}$ for all the clinical data sets were comparable (Supplemental Table 1).

Because the developed model was used to simulate PK of R- and S-carvedilol in both adult and pediatric populations and as reported in most PBPK model base studies (Johnson et al., 2006; De Buck et al., 2007; Li et al., 2012; Khalil and Laer, 2014), a twofold error range was used for evaluation of observed and predicted PK parameters.

Moreover, to identify any systemic error associated with predictions of R- and S-carvedilol, population predicted versus population observed plots with a twofold error range were used.

Results

Healthy Adults

The model predictions after i.v. and oral application in healthy adults were in good agreement with the observed data at all administered dosages of 12.5 mg i.v. and 6.4–50 mg oral racemic carvedilol (Fig. 2). The ratios$_{(Obs/Pred)}$ for $AUC_{0-\infty}$, C_{max}, and CL after i.v. and oral administration of R- and S-carvedilol were within twofold error range (Fig. 3). After i.v. administration, the systemic concentration of R-carvedilol was slightly higher than that of S-carvedilol, which was evident from a mean R/S $AUC_{0-\infty}$ ratio of 1.2 and 1.4 for observed and predicted data, respectively. An increase in the mean observed and predicted R/S $AUC_{0-\infty}$ ratios was seen after oral administration of carvedilol, as it was increased to 2.5 and 2.4, respectively, suggesting that stereoselective disposition is more pronounced after oral administration.

The visual predictive checks in EMs and PMs of CYP2D6 show that the model has slightly overpredicted the absorption phase (C_{max}) for S-carvedilol, but, for R-carvedilol, the C_{max} predictions were in agreement with the observed data (Fig. 2). The ratios$_{(Obs/Pred)}$ for all the PK parameters in EMs and PMs of CYP2D6 were within twofold

TABLE 2

Characteristics of the adult data sets used for carvedilol model development

No.	Population	No. of Subjects	Dose (mg)	Application	Age (years)		Body Weight (kg)		Ref.
					Mean	Range	Mean	Range	
1	Healthy	10[a]	12.5	i.v. infusion[b]	29.5	21–39	73.9	56.5–98	(Neugebauer et al., 1990)
2	Healthy	3	12.5	i.v. infusion[b]	—	—	—	—	(Spahn et al., 1990)
3	Healthy	10[a]	50	Oral	29.5	21–39	73.9	56.5–98	(Neugebauer et al., 1990)
4	Healthy	3	50	Oral	—	—	—	—	(Spahn et al., 1990)
5	Healthy	9	25	Oral	28.4[c]	—	82.1[c]	—	(Zhou and Wood, 1995)
6	Healthy	7	25	Oral	32[d]	—	89.0[d]	—	(Zhou and Wood, 1995)
7	Healthy	7	6.4[e]	Oral	29.7	24–37	71	56–100	(Behn, 2001)
8	Heart failure[f,g]	20	6.25	Oral	55	39–64	89.5	60.8–113.1	(Tenero et al., 2000)
9	Heart failure[f,g]	20	12.5	Oral	55	39–64	89.5	60.8–113.1	
10	Heart failure[f,g]	20	25	Oral	55	39–64	89.5	60.8–113.1	
11	Heart failure[f,g]	20	50	Oral	55	39–64	89.5	60.8–113.1	

[a]The number of patients included in pharmacokinetic analysis of S-carvedilol after i.v. and oral application were 6 and 7, respectively.
[b]Intravenous infusion was given over 1 hour.
[c]S.E.M. for age ±1.3 years and for weight ±3.2 kg.
[d]S.E.M. for age ±2.4 years and for weight ±6.9 kg.
[e]Dose administered as 0.09 mg/kg but normalized to total dose by multiplying with the average weight of the participants in the clinical trial.
[f]Twenty patients completed the study (10 patients with NYHA III and 10 with NYHA IV heart failure).
[g]The presented values for age and weight are the reported values for the initial study population ($n = 22$).

TABLE 3
Characteristics of pediatric data used for model development

No.	Age (years)	Gender	Body Weight (kg)	Dose (mg/kg)	Ross Score/NYHA Class
1	0.12	Female	3.1	0.09	3
2	0.13	Male	4	0.09	6
3	0.15	Male	3.9	0.09	3
4	0.5	Female	5.2	0.09	8
5	0.75	Male	8	0.09	3
6	1.25	Male	10.1	0.09	3
7	1.5	Male	9.5	0.09	10
8	3.5	Female	13.1	0.09	3
9	5.5	Male	20.2	0.09	3
10	7.5	Male	24.3	0.09	5
11	8.25	Male	25.8	0.09	7
12	11.6	Female	34.3	0.09	4
13	11.8	Male	39	0.09	2
14	17.5	Male	56	0.09	NYHA II
15	17.8	Male	61	0.09	NYHA III
16	19.3[a]	Male	98.2	0.09	NYHA III
Mean	6.7		26	—	—
S.D.	6.72		25.6	—	—

All patients were diagnosed with heart failure and were participants in the same clinical trial (Behn, 2001).
[a]Patient out of the pediatric age range according to guidelines set by World Health Organization.

error range (Fig. 3). Furthermore, the predicted versus observed systemic drug concentration plots after i.v. and oral application of R- and S-carvedilol showed that the model has successfully predicted the observed data at high and low systemic drug concentrations (Supplemental Fig. 3).

The predicted steady state volumes of distribution were 1.57 and 1.95 L/kg for R- and S-carvedilol, which are in line with reported values (range) of 1.39–3.40 and 1.42–3.84 L/kg, respectively. Additionally, the predicted bioavailability of R- and S-carvedilol in healthy adults was 0.34 and 0.17, respectively, which is in agreement with the reported absolute bioavailability of these enantiomers (Table 4).

Adult CHF Patients

The developed adult CHF model was successful in predicting stereoselective disposition of R- and S-carvedilol after administering steady state oral doses of racemic carvedilol (6.25–50 mg) in CHF patients (Fig. 4). The mean ratios$_{(Obs/Pred)}$ of the PK parameters for both enantiomers were within twofold error range and close to unity. The mean ratios$_{(Obs/Pred)}$ for $AUC_{0-\infty}$ and CL/F were 1.2 and 0.8 for R-carvedilol and 1.1 and 0.9 for S-carvedilol (Fig. 5). Moreover, the predicted versus observed systemic drug concentration plots in CHF showed that the model has successfully predicted steady state systemic concentrations of R- and S-carvedilol at all dosage levels (Supplemental Fig. 3). In adult with CHF, the mean R/S $AUC_{0-\infty}$ ratios were reduced to 1.8 and 1.6 for observed and predicted data, respectively, showing a relative increase in S-carvedilol concentration in CHF patients.

A decrease in predicted bioavailability (F) of both R- and S-carvedilol was seen in CHF patients, which was associated with decrease in f_a and F_h. The predicted f_a, F_h, and F in adult CHF patients were reduced to 0.74, 0.19, and 0.14 for R-carvedilol and to 0.55, 0.11, and 0.05 for S-carvedilol (Table 4).

Pediatric CHF Patients

The systemic concentration-time profiles of R- and S-carvedilol after administering an oral dose of 0.09 mg/kg racemic carvedilol in the entire age range (0.12–19.3 years) without incorporating any pathophysiological changes show that the developed model was capable of predicting the age-specific changes in systemic concentrations of both enantiomers, because most of the observed systemic concentration-time profiles were within predicted 5th and 95th percentiles (Supplemental Fig. 4).

Moreover, the age-related changes occurring in CL/F of R- and S-carvedilol were captured by the model, as the observed values were within the predicted CL/F range, except in two patients with age of 17.5 and 19.3 years, where the observed CL/F was lower than the predicted values (Supplemental Fig. 4).

The predicted systemic concentration-time profiles and the ratios$_{(Obs/Pred)}$ of the PK parameters in different pediatric age groups after administering an oral dose of 0.09 mg/kg racemic carvedilol are shown in Figs. 6 and 7. The infants, young children, and children who were classified with respect to Ross score were better described without incorporating pathophysiological changes in the model, as the $AUC_{0-\infty}$ and CL/F ratios$_{(Obs/Pred)}$ were always within twofold error range and the results in these age groups are as follows: In infants, the model has slightly overpredicted systemic concentration of both enantiomers that can be seen in the ratios$_{(Obs/Pred)}$ for C_{max} and $AUC_{0-\infty}$, which were 0.8 for R-carvedilol and 0.7 for S-carvedilol. The predictions in young children for R-carvedilol were in close agreement with the observed data, but the C_{max} for S-carvedilol was overpredicted in this age group and the $AUC_{0-\infty}$ ratios$_{(Obs/Pred)}$ for R- and S-carvedilol were 1.2 and 1.7, respectively. In children, the predictions for both enantiomers were in agreement with the observed data, and the CL/F and C_{max} ratios$_{(Obs/Pred)}$ for R and S carvedilol were 1.1 and 1.2, respectively (Figs. 6 and 7).

Among the three patients (two adolescents and one young adult) who were classified as adults, according to NYHA functional classification, two (17.5 and 19.3 years) were better described with incorporation of the pathophysiological changes, as in adults with CHF, and are presented individually in the visual predictive checks and comparison of PK parameters (Figs. 6 and 7). The 17.5-year-old patient classified as NYHA class II was better described with organ blood flow reductions as the ratios$_{(Obs/Pred)}$ for $AUC_{0-\infty}$ and CL/F without reduction in organ blood flows were outside the twofold error range, but with incorporation of adult organ blood flow reductions they were improved and were within twofold error range (Fig. 7). The 17.8-year-old patient classified as NYHA class III was better described without reductions in organ blood flows. The organ blood flow reductions in 19.3-year young adult classified as NYHA class III significantly improved the predictions as the ratios$_{(Obs/Pred)}$ for CL/F and C_{max} without reductions in blood flow were 0.6 and 3.2 for R-carvedilol and 0.3 and 4.7 for S-carvedilol and were improved to 1.7 for R-carvedilol and 1.5 and 1.4 for S-carvedilol, respectively (Fig. 7).
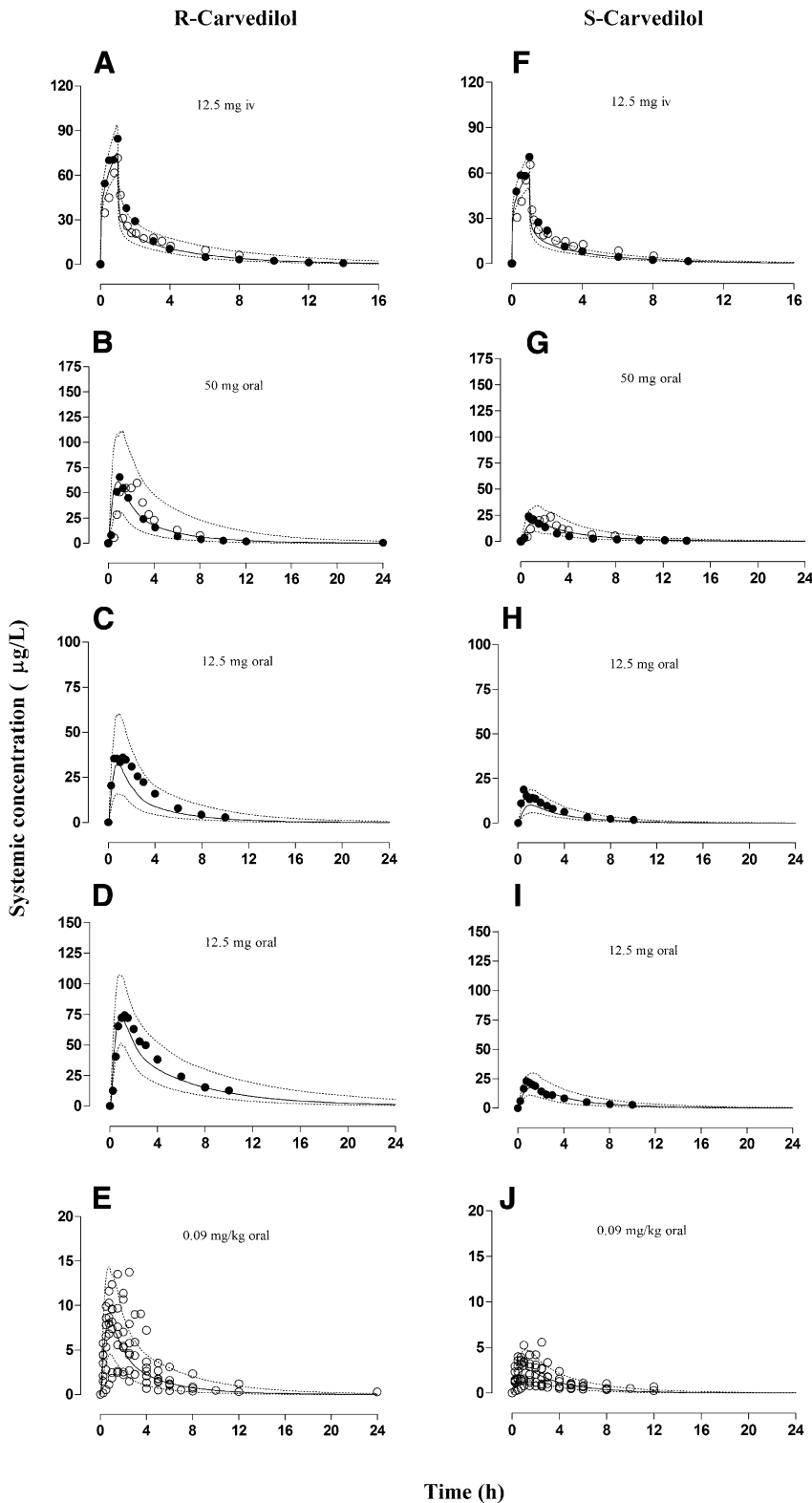
R-Carvedilol   **S-Carvedilol**

Fig. 2. Comparison of observed and predicted systemic R- and S-carvedilol concentration-time profiles in healthy adults after i.v. or oral drug dosing. Healthy adults, i.v. application (A, F) 12.5 mg, ● (Neugebauer et al., 1990), ○ (Spahn et al., 1990). Oral application, (B, G) 50 mg, ● (Neugebauer et al., 1990), ○ (Spahn et al., 1990), 25 mg (Zhou and Wood, 1995), (C, H) extensive metabolizers, (D, I) poor metabolizers, and (E, J) 0.09 mg/kg, $n = 7$ (Behn, 2001). Prediction results are shown as median (lines) and 5th and 95th percentiles (dotted lines). The observed data are shown as filled and empty circles.

Lastly, the predicted versus observed systemic drug concentration plots in pediatrics show that, with few exceptions, particularly with R-carvedilol, where model has underpredicted the systemic concentrations, in general the model was capable of predicting the individual concentrations of both enantiomers, as most of the concentrations were within twofold error range (Supplemental Fig. 5).

Discussion

In the presented work, the pathophysiological organ blood flow changes occurring in CHF were incorporated into whole-body PBPK model to predict stereoselective disposition of carvedilol in CHF patients. When the developed PBPK model has successfully described PK of R- and S-carvedilol in healthy adults and after incorporation of
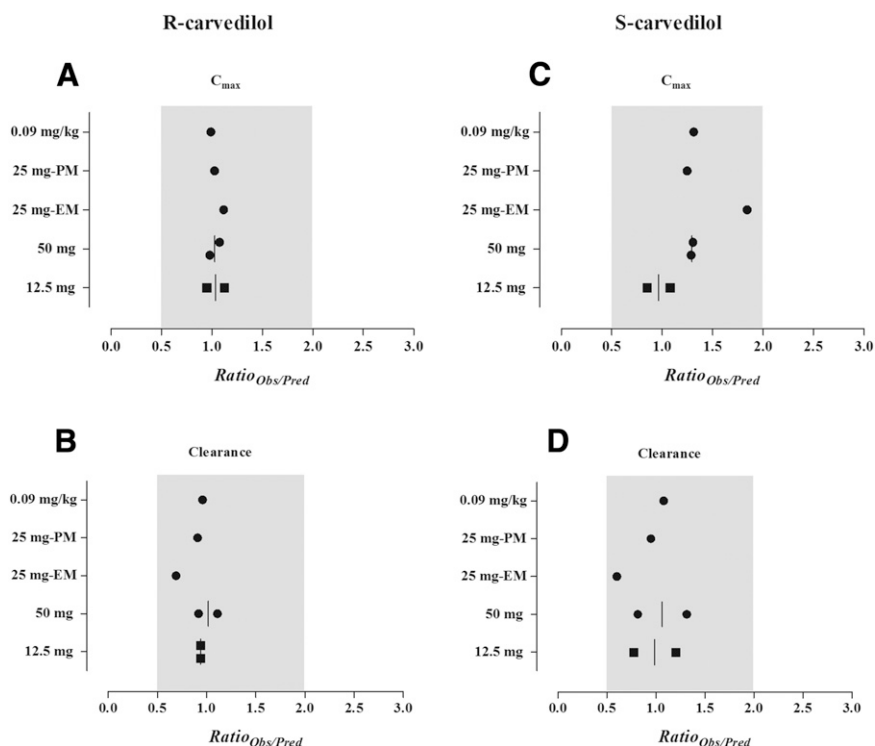
R-carvedilol   S-carvedilol

Fig. 3. Comparison between the observed and predicted values of $AUC_{0-\infty}$, C_{max}, and drug clearance in healthy adults. Results are presented as ratios$_{(Obs/Pred)}$. (A, B) R-carvedilol and (C, D) S-carvedilol ● oral application, ■ i.v. application. The shadowed gray area indicates a twofold error range. When more than one clinical observed data were available at the same dose level, a line was used to show the mean of the ratio$_{(Obs/Pred)}$. CL is the calculated CL/F if the dose is given orally.

reduced organ blood flows in adult CHF patients, it was scaled to pediatric CHF patients. The scaling of adult model to children helped in exploring whether the same pathophysiological changes seen in adult CHF patients could be adopted for the pediatric CHF patients.

The model development was initiated by parameterization of various drug-specific parameters after i.v. application in healthy adults, which was followed by predictions of R- and S-carvedilol after oral administration. The predicted bioavailability of R- and S-carvedilol was in very close agreement with the reported absolute bioavailability of these enantiomers (Neugebauer et al., 1990) (Table 4). The additional success in predicting the disposition of R- and S-carvedilol in EMs and PMs of CYP2D6 provided additional confidence in the CYP2D6 CL_{int} values used in the developed model, as this enzyme is the most relevant for the drug metabolism. Moreover, in comparison with R-carvedilol, the slight overprediction of C_{max} with S-carvedilol highlights the equally important role of other cyp-enzymes involved in its metabolism, as in the developed model only 50% CL of S-carvedilol is attributed to CYP2D6 and remaining 30% to other cyp-enzymes, whereas with R-carvedilol 74% CL is associated with CYP2D6 and remaining 6% is attributed to other cyp-enzymes. Therefore, this suggests that, in addition to CYP2D6 gentotype, the incorporation of genotype-specific data for other

cyp-enzymes involved in CL of S-carvedilol is equally important for predicting its ADME.

The developed model was successful in predicting the ~twofold difference in F of both enantiomers (Table 4). It was seen that carvedilol undergoes extensive stereoselective first-pass metabolism that is more sensitive toward S-carvedilol. Furthermore, the resulted R/S $AUC_{0-\infty}$ ratios suggest that stereoselective CL of carvedilol is more distinct after oral administration, because the predicted R/S $AUC_{0-\infty}$ ratio in healthy adults after i.v. administration was 1.4 and it was increased to 2.4 after oral administration of carvedilol. The predicted R/S $AUC_{0-\infty}$ ratio was decreased to 1.6 in adult CHF patients after administering steady state oral application of carvedilol. This decrease in R/S $AUC_{0-\infty}$ ratio was associated with differences in CL_{int} of both enantiomers, as the reduction of Q_H in CHF resulted in a differential effect on CL of both enantiomers. Therefore, in CHF compared with R-carvedilol, there will be a relative increase in S-carvedilol systemic concentration and hence its $AUC_{0-\infty}$. This relative increase in S-carvedilol exposure is expected to expand with increased severity of disease.

The incorporation of reduced blood flows to liver and kidney in adult CHF patients resulted in decreased CL/F of R- and S-carvedilol; because both carvedilol enantiomers undergo extensive first-pass metabolism

TABLE 4

Predicted bioavailability of carvedilol enantiomers in different populations

Simulated Population	R-Carvedilol				S-Carvedilol			
	F_g	F_h	f_a	F	F_g	F_h	f_a	F
Healthy adults	0.98	0.35	0.99	0.34	0.96	0.21	0.88	0.17
Extensive metabolizers	0.99	0.35	0.99	0.34	0.96	0.20	0.89	0.17
Poor metabolizers	1.00	0.65	0.99	0.64	0.98	0.34	0.89	0.30
Adults with heart failure	0.97	0.19	0.74	0.14	0.92	0.11	0.55	0.05
Pediatrics with heart failure[a]	0.98	0.42	0.99	0.41	0.96	0.27	0.93	0.23

F, bioavailability; f_a, fraction of drug absorbed; F_g, fraction of drug escaping metabolism in the gut; F_h, fraction of drug escaping the hepatic metabolism.
[a]Simulation performed without reducing organ blood flows.
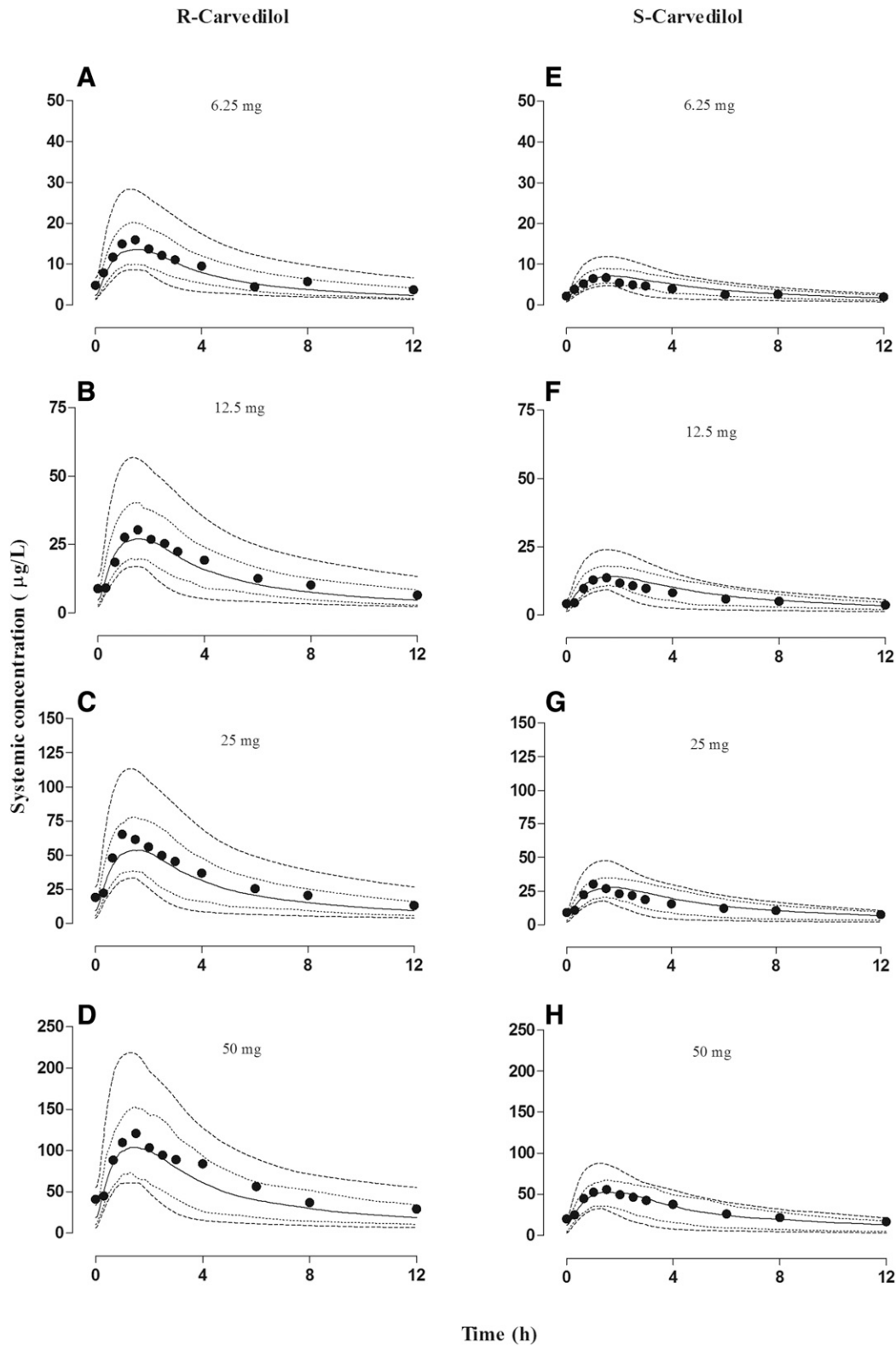
R-Carvedilol

S-Carvedilol

Fig. 4. Comparison of observed and predicted systemic R- and S-carvedilol concentration-time profiles after steady state oral drug dosing in heart failure patients: (A, E) 6.25 mg, (B, F) 12.5 mg, (C, G) 25 mg, and (D, H) 50 mg oral carvedilol. Observed data are shown as dark circles (Tenero et al., 2000). Prediction results are shown as median (lines), 5th and 95th percentiles (dotted lines), and minimum/maximum (dashed lines).

(Neugebauer et al., 1990), this decrease in CL/F was primarily attributed to reduction in Q_H. The reduced Q_H led to an increased first-pass metabolism (decrease in F_h), which, in turn, resulted in reduced F of both enantiomers. The decrease in carvedilol CL/F and F was successfully predicted by the developed model in CHF patients (Figs. 4 and 5; Table 4). Furthermore, the predicted f_a of both enantiomers was reduced in adult CHF patients (Table 4), which is consistent with the reports stating reduction in passive drug diffusion is due to reduction in Q_{villi} in
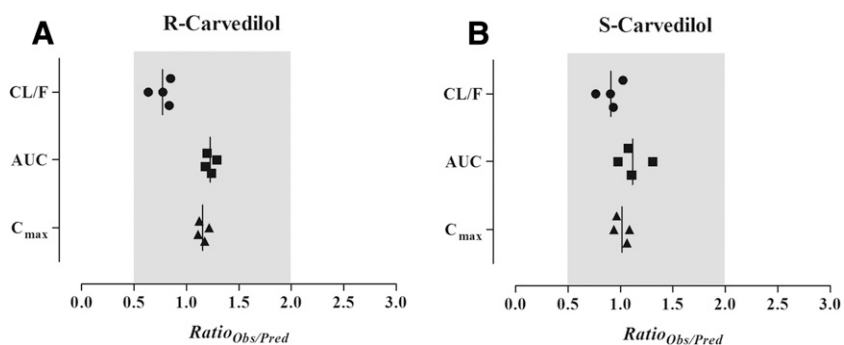
Fig. 5. Comparison between the observed and predicted values of $AUC_{0-\infty}$ ■, C_{max} ▲, and CL/F ● in adult heart failure population. Results are presented as mean ratios$_{(Obs/Pred)}$ for R-carvedilol (A) and S-carvedilol (B).

CHF (Berkowitz et al., 1963; Sica, 2003). Moreover, in CHF, the absorption of drugs with low solubility is more susceptible to changes in intestinal blood flow; therefore, for drugs like carvedilol (BCS class II) having low solubility and high permeability, any change in blood flow to intestine can have an impact on its f_a (Ogawa et al., 2014). In the developed model, due to absence of any clear information on the
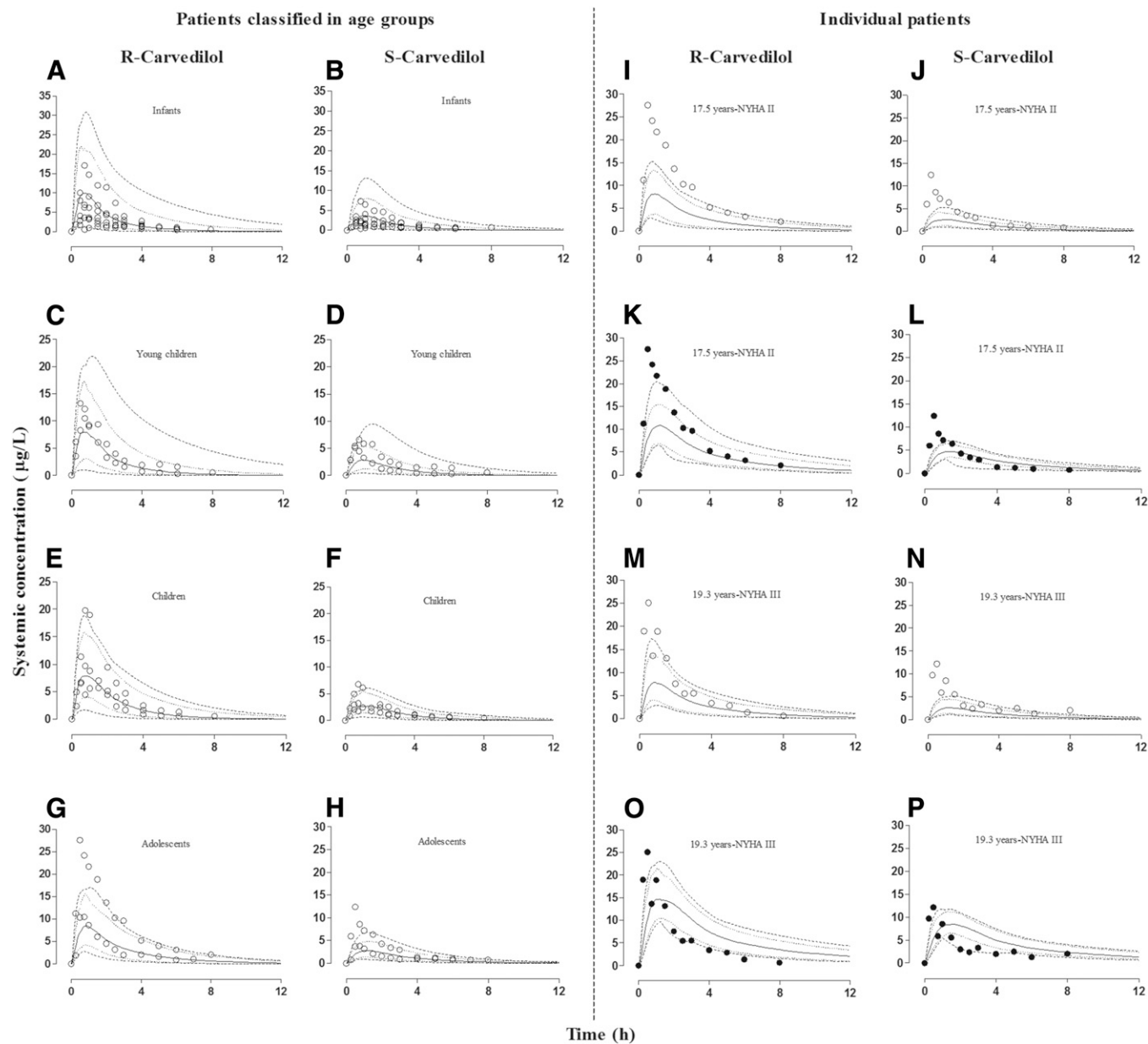
Fig. 6. Model predictions in different pediatric age groups for R- and S-carvedilol (A, B) infants, (C, D) young children, (E, F) children, and (G, H) adolescents. Model predictions in individual patients (I–P) after administering 0.09 mg/kg oral dose racemic carvedilol, without (○) and with (●) adjusting the organ blood flows, ── median prediction, ---- minimum and maximum prediction, ⋯ 5th and 95th percentiles, and ●, ○ observed data (Behn, 2001).
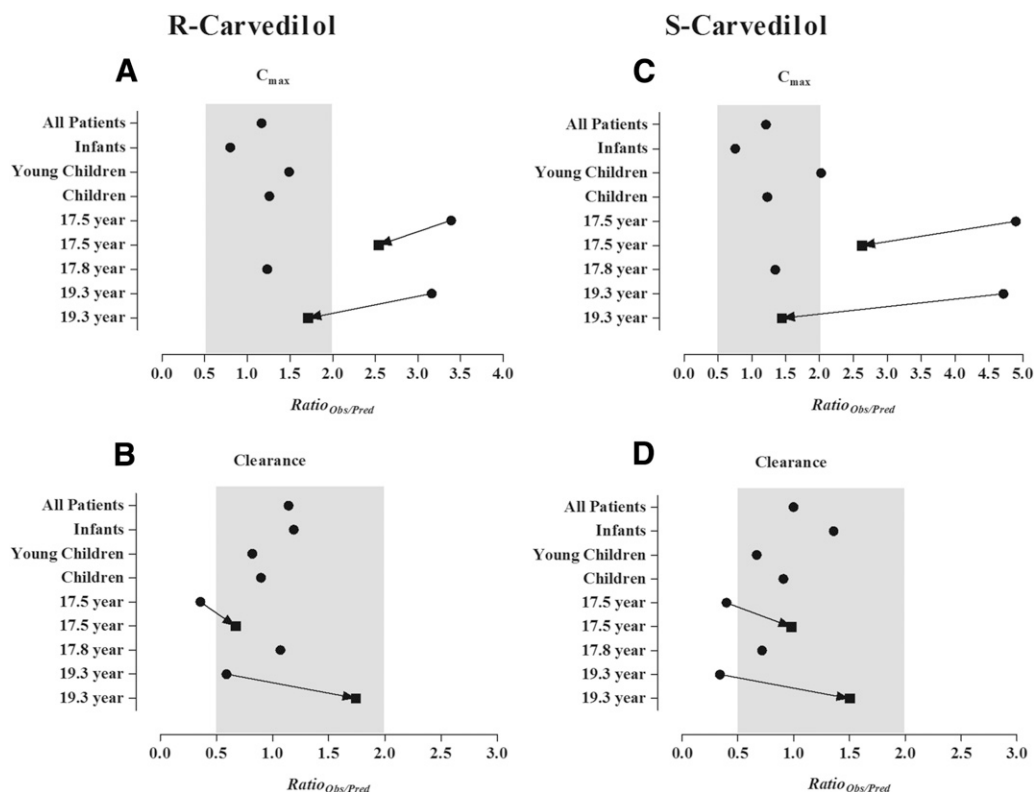
Fig. 7. Comparison between the observed and predicted values of C_{max} and CL/F in pediatric CHF patients. Results are presented as individual and ratios(Obs/Pred) (A, B) R-carvedilol and (C, D) S-carvedilol ● predictions without organ blood flow reductions and ■ predictions with incorporation of organ blood flow reductions. The arrowhead of the line points from ratio(Obs/Pred) without reduction in organ blood flow to ratio(Obs/Pred) with reduction in organ blood flow in the same patient. The shadowed gray area indicates a twofold error range.

intestinal blood flow in relation to severity of CHF, intestinal blood flow was not reduced with severity of CHF. Instead, reduction in Q_H was used as a surrogate; therefore, to account for decrease in Q_{villi} and its impact on absorption of both enantiomers, the Q_{Gut} was reduced in relation to reduction in Q_H.

The pediatric simulations showed that, in contrast to the adults, the patients up to 12 years of age, all categorized with Ross scoring system, were better described without the reductions in organ blood flow. In contrast, one from the two adolescent patients as well as the young adult patient (17.5 and 19.3 years, all classified according to NYHA classification) were better described after incorporating organ blood flow reductions. One of the possible reasons for such a difference may be the use of the same organ blood flow reductions in pediatric population as in adults. Because the incorporated blood flow reductions in pediatrics simulations were based on adult values, it is likely that these values might be close to what is happening in the late adolescence, but not be true for young children, as improvement in predictions with incorporation of reduced organ blood flows was only seen in old adolescents (the young adults). Moreover, the pathophysiology of CHF is different between adult and pediatric patients, with congenital heart disease being the main cause of CHF in the vast majority of pediatric patients (Hsu and Pearson, 2009). Compared with adults, children have higher frequency of heart rate (Tanaka et al., 2001; Fleming et al., 2011) and a higher drug CL due to higher percentage of liver weight in relation to body weight (Noda et al., 1997). This can lead to differences in the total impact of these changes on drug CL between both populations. In addition to that, it is not clear whether the different grading system that was used is related, in any way, to this finding, as both grading systems are based on different criteria. To draw conclusions about the validity of this finding as well as the possible reasons for it, more data are needed specially to confirm whether this difference is true. However, the presented findings indicate that the incorporated blood flow reductions in the adult model cannot be directly adopted in pediatrics, at least for the young ones.

The ontogeny of the metabolic cyp-enzymes seems to have a minor impact on the overall disposition of carvedilol enantiomers in the pediatric CHF patients that were included in the model evaluation (Behn, 2001). This is because all of these pediatric patients were above 1 month of age and the two major cyp-enzymes for carvedilol metabolism (i.e., CYP2D6 and CYP2C9) have a fast ontogeny profile, as they achieve more than ~50% of adult activity by the age of 0.1 year (Salem et al., 2013). Nevertheless, in the developed model, about 20% of the total assigned metabolism of S-carvedilol is due to cyp-enzymes with slow enzyme ontogeny and a later maturation time point, that is, CYP1A2, 10%; CYP2E1, 5%; and CYP3A4, 5%. The latter enzymes contribute only to about 4% in the case of R-carvedilol, that is, CYP1A2, 2%; CYP2E1, 1%; and CYP3A4, 1%. As a result, the impact of the slow maturation of these enzymes will be more profound on the CL of S- rather than the R-carvedilol. Moreover, if pediatric patients less than 1 month of age would have been included, the effect of enzyme ontogeny on the predicted drug CL would have been more pronounced.

The predicted systemic drug concentration profiles for R- and S-carvedilol in different pediatric age groups have successfully captured the observed data, with few exceptions, where model has overpredicted the systemic concentrations of R- and S-carvedilol, particularly in infants. These overpredictions in infants may be associated with the knowledge gaps with respect to intestinal permeability and perfusion within CHF patients of this age group, as low drug absorption in

comparison with adults has been previously reported in pediatric CHF due to congenital heart defects (Nakamura et al., 1994). Because changes in intestinal morphology, permeability, and absorption are affected in adult CHF patients, the possibility of such changes in pediatric CHF patients cannot be completely ruled out (Sica, 2003; Sandek et al., 2007).

The age-related changes in CL/F for R- and S-carvedilol have been successfully captured by the developed PBPK model (Supplemental Fig. 5). The observed CL/F values were within the predicted values, except in 17.5- and 19.3-year patients, where the observed CL/F for both enantiomers were low, which can be attributed to reduced blood supply to eliminating organs in these patients as only in these two patients, the predicted PK parameters were improved with incorporation of reduced organ blood flows (Fig. 7). Additionally, due to the higher hepatic extraction of S-carvedilol, the impact of reduction in Q_H on its CL/F was more significant when compared with R-carvedilol. However, it seems that the role of reduced organ blood flows becomes important only in adolescents, who were categorized according to NYHA classification of CHF. Because the number of participants in the clinical study used for model evaluation in pediatrics was small, these results cannot be generalized for all of the pediatric CHF patients.

Because the developed model has successfully predicted the stereoselective disposition of carvedilol in healthy and diseased populations, it can be used to predict genotype-specific CL/F in special populations (pediatrics, geriatrics, and cirrhosis) and can assist in improving the safety profile of carvedilol by reducing the adverse drug reactions associated with it, particularly the ones associated with higher systemic concentrations of R-carvedilol (orthostatic hypotension) that can lead to serious consequences in the geriatric population.

We will end by quoting G. T. Tucker and M. S. Lennard: "When looking glass drugs are given their PKs should, whenever possible, be viewed from both sides of the mirror" (Tucker and Lennard, 1990).

Acknowledgments

Authorship Contributions

Participated in research design: Rasool, Khalil, Läer.

Conducted experiments: Rasool.

Performed data analysis: Rasool, Khalil.

Wrote or contributed to the writing of the manuscript: Rasool, Khalil, Läer.

References

Aiba T, Ishida K, Yoshinaga M, Okuno M, and Hashimoto Y (2005) Pharmacokinetic characterization of transcellular transport and drug interaction of digoxin in Caco-2 cell monolayers. *Biol Pharm Bull* 28:114–119.

Behn F (2001) Pharmakokinetik, *Pharmakodynamik und Pharmakogenetik von Carvedilol in Abhängigkeit vom Lebensalter bei pädiatrischen Patienten mit Herzinsuffizienz*. Doctoral dissertation, Universität Hamburg, Hamburg, Germany.

Benet LZ, Broccatelli F, and Oprea TI (2011) BDDCS applied to over 900 drugs. *AAPS J* 13: 519–547.

Berezhkovskiy LM (2004) Volume of distribution at steady state for a linear pharmacokinetic system with peripheral elimination. *J Pharm Sci* 93:1628–1640.

Berkowitz D, Croll MN, and Likoff W (1963) Malabsorption as a complication of congestive heart failure. *Am J Cardiol* 11:43–47.

Birkett DJ (1989) Racemates or enantiomers: regulatory approaches. *Clin Exp Pharmacol Physiol* 16:479–483.

Caron G, Steyaert G, Pagliara A, Reymond F, Crivori P, Gaillard P, Carrupt P-A, Avdeef A, Comer J, and Box KJ, et al. (1999) Structure-Lipophilicity relationships of neutral and protonated β-blockers, part I, intra- and intermolecular effects in isotropic solvent systems. *Helv Chim Acta* 82:1211–1222.

Criteria Committee of the New York Heart Association (1994) *Nomenclature and Criteria for Diagnosis of Diseases of the Heart and Great Vessels*, Little, Brown, and Company, Boston.

Cubitt HE, Yeo KR, Howgate EM, Rostami-Hodjegan A, and Barter ZE (2011) Sources of interindividual variability in IVIVE of clearance: an investigation into the prediction of benzodiazepine clearance using a mechanistic population-based pharmacokinetic model. *Xenobiotica* 41: 623–638.

De Buck SS, Sinha VK, Fenu LA, Nijsen MJ, Mackie CE, and Gilissen RA (2007) Prediction of human pharmacokinetics using physiologically based modeling: a retrospective analysis of 26 clinically tested drugs. *Drug Metab Dispos* 35:1766–1780.

Fleming S, Thompson M, Stevens R, Heneghan C, Plüddemann A, Maconochie I, Tarassenko L, and Mant D (2011) Normal ranges of heart rate and respiratory rate in children from birth to 18 years of age: a systematic review of observational studies. *Lancet* 377:1011–1018.

Fujimaki M, Murakoshi Y, and Hakusui H (1990) Assay and disposition of carvedilol enantiomers in humans and monkeys: evidence of stereoselective presystemic metabolism. *J Pharm Sci* 79: 568–572.

Gehr TW, Tenero DM, Boyle DA, Qian Y, Sica DA, and Shusterman NH (1999) The pharmacokinetics of carvedilol and its metabolites after single and multiple dose oral administration in patients with hypertension and renal insufficiency. *Eur J Clin Pharmacol* 55: 269–277.

Giessmann T, Modess C, Hecker U, Zschiesche M, Dazert P, Kunert-Keil C, Warzok R, Engel G, Weitschies W, and Cascorbi I, et al. (2004) CYP2D6 genotype and induction of intestinal drug transporters by rifampin predict presystemic clearance of carvedilol in healthy subjects. *Clin Pharmacol Ther* 75:213–222.

Hsu DT and Pearson GD (2009) Heart failure in children: part I: history, etiology, and pathophysiology. *Circ Heart Fail* 2:63–70.

Jamei M, Turner D, Yang J, Neuhoff S, Polak S, Rostami-Hodjegan A, and Tucker G (2009) Population-based mechanistic prediction of oral drug absorption. *AAPS J* 11:225–237.

Johnson TN and Rostami-Hodjegan A (2011) Resurgence in the use of physiologically based pharmacokinetic models in pediatric clinical pharmacology: parallel shift in incorporating the knowledge of biological elements and increased applicability to drug development and clinical practice. *Paediatr Anaesth* 21:291–301.

Johnson TN, Rostami-Hodjegan A, and Tucker GT (2006) Prediction of the clearance of eleven drugs and associated variability in neonates, infants and children. *Clin Pharmacokinet* 45: 931–956.

Kaijser M, Johnsson C, Zezina L, Backman U, Dimény E, and Fellström B (1997) Elevation of cyclosporin A blood levels during carvedilol treatment in renal transplant patients. *Clin Transplant* 11:577–581.

Khalil F and Läer S (2014) Physiologically based pharmacokinetic models in the prediction of oral drug exposure over the entire pediatric age range: sotalol as a model drug. *AAPS J* 16: 226–239.

Läer S, Mir TS, Behn F, Eiselt M, Scholz H, Venzke A, Meibohm B, and Weil J (2002) Carvedilol therapy in pediatric patients with congestive heart failure: a study investigating clinical and pharmacokinetic parameters. *Am Heart J* 143:916–922.

Lee R, Beard J, and Aldoori M (1993) Blood flow to the limbs, in *Cardiac Output and Regional Flow in Health and Disease* (Salmasi A-M and Iskandrian A eds) pp 505–522, Springer, Dordrect, The Netherlands.

Leithe ME, Margorien RD, Hermiller JB, Unverferth DV, and Leier CV (1984) Relationship between central hemodynamics and regional blood flow in normal subjects and in patients with congestive heart failure. *Circulation* 69:57–64.

Li GF, Wang K, Chen R, Zhao HR, Yang J, and Zheng QS (2012) Simulation of the pharmacokinetics of bisoprolol in healthy adults and patients with impaired renal function using whole-body physiologically based pharmacokinetic modeling. *Acta Pharmacol Sin* 33: 1359–1371.

Nakamura H, Ishii M, Sugimura T, Chiba K, Kato H, and Ishizaki T (1994) The kinetic profiles of enalapril and enalaprilat and their possible developmental changes in pediatric patients with congestive heart failure. *Clin Pharmacol Ther* 56:160–168.

Neugebauer G, Akpan W, Kaufmann B, and Reiff K (1990) Stereoselective disposition of carvedilol in man after intravenous and oral administration of the racemic compound. *Eur J Clin Pharmacol* 38 (Suppl 2):S108–S111.

Neugebauer G and Neubert P (1991) Metabolism of carvedilol in man. *Eur J Drug Metab Pharmacokinet* 16:257–260.

Noda T, Todani T, Watanabe Y, and Yamamoto S (1997) Liver volume in children measured by computed tomography. *Pediatr Radiol* 27:250–252.

Ogawa R, Stachnik JM, and Echizen H (2013) Clinical pharmacokinetics of drugs in patients with heart failure: an update (part 1, drugs administered intravenously). *Clin Pharmacokinet* 52: 169–185.

Ogawa R, Stachnik JM, and Echizen H (2014) Clinical pharmacokinetics of drugs in patients with heart failure: an update (part 2, drugs administered orally). *Clin Pharmacokinet* 53:1083–1114.

Ohno A, Saito Y, Hanioka N, Jinno H, Saeki M, Ando M, Ozawa S, and Sawada J (2004) Involvement of human hepatic UGT1A1, UGT2B4, and UGT2B7 in the glucuronidation of carvedilol. *Drug Metab Dispos* 32:235–239.

Oldham HG and Clarke SE (1997) In vitro identification of the human cytochrome P450 enzymes involved in the metabolism of R(+)- and S(-)-carvedilol. *Drug Metab Dispos* 25:970–977.

Rasool MF, Khalil F, and Läer S (2015) A physiologically based pharmacokinetic drug-disease model to predict carvedilol exposure in adult and paediatric heart failure patients by incorporating pathophysiological changes in hepatic and renal blood flows. *Clin Pharmacokinet* 54:943–962.

Ross RD, Bollinger RO, and Pinsky WW (1992) Grading the severity of congestive heart failure in infants. *Pediatr Cardiol* 13:72–75.

Salem F, Johnson TN, Abduljalil K, Tucker GT, and Rostami-Hodjegan A (2014) A re-evaluation and validation of ontogeny functions for cytochrome P450 1A2 and 3A4 based on in vivo data. *Clin Pharmacokinet* 53:625–636.

Salem F, Johnson TN, Barter ZE, Leeder JS, and Rostami-Hodjegan A (2013) Age related changes in fractional elimination pathways for drugs: assessing the impact of variable ontogeny on metabolic drug-drug interactions. *J Clin Pharmacol* 53:857–865.

Sandek A, Bauditz J, Swidsinski A, Buhner S, Weber-Eibel J, von Haehling S, Schroedl W, Karhausen T, Doehner W, and Rauchhaus M, et al. (2007) Altered intestinal function in patients with chronic heart failure. *J Am Coll Cardiol* 50:1561–1569.

Sehrt D, Meineke I, Tzvetkov M, Gültepe S, and Brockmöller J (2011) Carvedilol pharmacokinetics and pharmacodynamics in relation to CYP2D6 and ADRB pharmacogenetics. *Pharmacogenomics* 12:783–795.

Sica DA (2003) Pharmacotherapy in congestive heart failure: drug absorption in the management of congestive heart failure: loop diuretics. *Congest Heart Fail* 9:287–292.

Spahn H, Henke W, Langguth P, Schloos J, and Mutschler E (1990) Measurement of carvedilol enantiomers in human plasma and urine using S-naproxen chloride for chiral derivatization. *Arch Pharm* 323:465–469.

Takekuma Y, Yagisawa K, and Sugawara M (2012) Mutual inhibition between carvedilol enantiomers during racemate glucuronidation mediated by human liver and intestinal microsomes. *Biol Pharm Bull* **35**:151–163.

Tanaka H, Monahan KD, and Seals DR (2001) Age-predicted maximal heart rate revisited. *J Am Coll Cardiol* **37**:153–156.

Tenero D, Boike S, Boyle D, Ilson B, Fesniak HF, Brozena S, and Jorkasky D (2000) Steady-state pharmacokinetics of carvedilol and its enantiomers in patients with congestive heart failure. *J Clin Pharmacol* **40**:844–853.

Tian Y, He Y, Hu H, Wang L, and Zeng S (2012) Determination of the enantioselectivity of six chiral aryloxy aminopropanol drugs transport across Caco-2 cell monolayers. *Acta Pharm Sin B* **2**:168–173.

Tucker GT and Lennard MS (1990) Enantiomer specific pharmacokinetics. *Pharmacol Ther* **45**:309–329.

Wessler JD, Grip LT, Mendell J, and Giugliano RP (2013) The P-glycoprotein transport system and cardiovascular drugs. *J Am Coll Cardiol* **61**:2495–2502.

Wilkinson GR and Shand DG (1975) Commentary: a physiological approach to hepatic drug clearance. *Clin Pharmacol Ther* **18**:377–390.

Yancy CW, Jessup M, Bozkurt B, Butler J, Casey DE, Jr, Drazner MH, Fonarow GC, Geraci SA, Horwich T, and Januzzi JL, et al. (2013) 2013 ACCF/AHA guideline for the management of heart failure: executive summary: a report of the American College of Cardiology Foundation/American Heart Association Task Force on practice guidelines. *Circulation* **128**:1810–1852.

Zelis R, Nellis SH, Longhurst J, Lee G, and Mason DT (1975) Abnormalities in the regional circulations accompanying congestive heart failure. *Prog Cardiovasc Dis* **18**:181–199.

Zhou HH and Wood AJ (1995) Stereoselective disposition of carvedilol is determined by CYP2D6. *Clin Pharmacol Ther* **57**:518–524.

Address correspondence to: Muhammad Fawad Rasool, Department of Clinical Pharmacy and Pharmacotherapy, Heinrich-Heine University, 40225 Düsseldorf, Germany. E-mail: fawadrasool@bzu.edu.pk; fawad.rasool@uni-duesseldorf.de